



HAL
open science

High-frequency forced oscillations in neuronlike elements

Denis Zakharov, Martin Krupa, Boris Gutkin, Alexey Kuznetsov

► **To cite this version:**

Denis Zakharov, Martin Krupa, Boris Gutkin, Alexey Kuznetsov. High-frequency forced oscillations in neuronlike elements. *Physical Review E*, 2018, 97 (6), 10.1103/PhysRevE.97.062211 . hal-01962910

HAL Id: hal-01962910

<https://inria.hal.science/hal-01962910>

Submitted on 13 Mar 2024

HAL is a multi-disciplinary open access archive for the deposit and dissemination of scientific research documents, whether they are published or not. The documents may come from teaching and research institutions in France or abroad, or from public or private research centers.

L'archive ouverte pluridisciplinaire **HAL**, est destinée au dépôt et à la diffusion de documents scientifiques de niveau recherche, publiés ou non, émanant des établissements d'enseignement et de recherche français ou étrangers, des laboratoires publics ou privés.

High-frequency forced oscillations in neuronlike elementsD. G. Zakharov,¹ M. Krupa,² B. S. Gutkin,^{3,4} and A. S. Kuznetsov^{5,*}¹*Institute of Applied Physics of RAS, 46 Ulyanov Str., Nizhny Novgorod, Russia*²*Laboratoire Jean-Alexandre Dieudonné, Université de Côte d'Azur, Nice, France*³*Group of Neural Theory, LNC INSERM U960, École Normale Supérieure PSL* University, 29 rue d'Ulm, Paris, France*⁴*Centre for Cognition and Decision Making, National Research University Higher School of Economics, Myasnitskaya St. 20, Moscow, Russia*⁵*Department of Mathematical Sciences and Center for Mathematical Modeling and Computational Sciences, Indiana University–Purdue University Indianapolis, 402 N. Blackford St., Indianapolis, Indiana 46202, USA*

(Received 13 December 2017; revised manuscript received 25 March 2018; published 18 June 2018)

We analyzed a generic relaxation oscillator under moderately strong forcing at a frequency much greater than the natural intrinsic frequency of the oscillator. Additionally, the forcing is of the same sign and, thus, has a nonzero average, matching neuroscience applications. We found that, first, the transition to high-frequency synchronous oscillations occurs mostly through periodic solutions with virtually no chaotic regimes present. Second, the amplitude of the high-frequency oscillations is large, suggesting an important role for these oscillations in applications. Third, the 1:1 synchronized solution may lose stability, and, contrary to other cases, this occurs at smaller, but not at higher frequency differences between intrinsic and forcing oscillations. We analytically built a map that gives an explanation of these properties. Thus, we found a way to substantially “overclock” the oscillator with only a moderately strong external force. Interestingly, in application to neuroscience, both excitatory and inhibitory inputs can force the high-frequency oscillations.

DOI: [10.1103/PhysRevE.97.062211](https://doi.org/10.1103/PhysRevE.97.062211)**I. INTRODUCTION**

Oscillators under the influence of external forcing have been studied for several decades [1]. The problem has a very diverse list of applications, from phase-locked generators [2] to complex oscillatory [3] and neural networks [4]. Many systems display synchronization at the frequency of forcing and its $n : m$ multiples ($n > m$ ultraharmonics and $m > n$ subharmonics). Depending on the forcing strength and the mismatch of forcing and intrinsic frequencies, synchronization at different frequencies constitute the classical picture of Arnold’s tongues [5]: regions of synchrony tapering down with decreasing amplitude of forcing. The width of the regions is greater if the forcing and the intrinsic frequencies are similar. However, most of the research, especially analytical techniques, has been focused on the case of weak forcing and small to moderate frequency mismatch (for example, phase oscillators and integrate-and-fire neurons [6–8] are designed for this case).

Yet, in a number of applications, forcing is not weak but is moderately strong, and the intrinsic frequency is very different from the forcing frequency [9–11]. Dynamics of oscillators under such forcing, and especially the transition from low- to high-frequency oscillations are not well understood, and that is the case we consider here [12–15].

Note that the case of moderately strong periodic high-frequency input may appear in a wide class of networks, such as multiplex networks which are sets of elements with coupled layered topology (see, e.g., [12]). Each layer of such

a system may have different elements, different topologies, or different dynamical features of the elements. If, for example, the elements of a fast layer transiently synchronize, they are able to provide a strong high-frequency input to a slower layer. Such situation could be widely observed in the brain, where often a low-frequency neuron is driven by high-frequency input [16–18]. One can treat multiple neuron types as intrinsic oscillators and their electrical activity can be described by models with periodic, limit cyclelike behavior [19]. Simultaneously, they receive numerous inputs from neural populations that can transiently synchronize to produce strong pulses at a high frequency [20]. Thus in this paper, we model a situation general for many neuron types under external inputs.

In our previous biophysical modeling study [17], where interaction between two neuronal networks in the ventral tegmental area was studied, we found a surprising increase in the frequency of a slower neuron driven by a pulsatile *inhibitory* input. Thus, the influence of an inhibitory neuronal network on a neuron’s firing pattern may differ significantly from the traditionally considered decrease in the firing frequency of the target neuron. In fact, should this afferent inhibitory network synchronize, it may unintuitively lead to an increase in the target neuron response. Thus, this effect depends on the temporal structure of the inhibitory afferents (their synchrony, amplitude, and frequency), but may also depend on the intrinsic properties of the target neuron. The present paper defines these properties by reproducing the increase in the neuron response in a highly simplified model with only basic neural characteristics.

In that previous study, the target neuron was modeled by the conductance-based Hodgkin-Huxley model with specific currents for a particular type of neuron (dopaminergic, DA,

*zakharov@neuron.appl.sci-nnov.ru

neuron). The DA neuron is a slow pacemaker that cannot be driven to high frequencies with a tonic (constant) excitatory drive, and the model reflects this limitation. The neuron receives inputs at a much higher frequency than the intrinsic frequency. These inputs are for most of the time asynchronous, resulting in a near-constant input tone. Yet, during behaviorally relevant episodes they synchronize transiently, resulting in sharp relatively large amplitude “negative” input pulses. We have found that the neuron is capable of following this pulsatile drive. The transition to forced oscillations is well known, but this result is surprising because of two distinctions: First, in generic cases, the amplitude of forced oscillations is usually small at high forcing frequencies, which renders them insignificant for applications. In our case, the forced oscillation amplitude remains high and contributes to brain information coding by initiation of spikes. Second, the pulsatile input comes from an inhibitory population, yet it excites the DA neuron (i.e., increases its frequency). Transition to 1:1 synchronization occurs through a series of periodic solutions with periods that are integer multiples of the forcing period: As the forcing strength increases, the locking number decreases by one (e.g., 4:1, 3:1, 2:1, 1:1). Contrary to the classical results, the amplitude of these oscillations is not decreasing, and the 1:1 synchronous fast oscillation has a large amplitude, as in our neuron model [17]. Once 1:1 synchronization is established, it may lose stability in another bifurcation transition—period doubling [21], and, contrary to intuition, the loss of stability occurs at smaller, but not at higher frequency differences between intrinsic and forcing oscillations. The explanation and generalization of this regime are given below.

II. MODEL

We looked for a general oscillator model which can qualitatively describe a spiking neuron in the most general case. We thus consider a relaxation oscillator with an N-shaped nullcline under the influence of high-frequency forcing. As a general example, we take the two-dimensional McKean system [22], which is a piecewise linear analog of the FitzHugh-Nagumo model:

$$\begin{aligned} du/dt &= f(u) - v + \varphi(t), \\ dv/dt &= \epsilon(u - k), \end{aligned} \quad (1)$$

$$f(u) = \begin{cases} -u, & u \leq 0.25, \\ u - 0.5, & 0.25 < u \leq 0.75, \\ 1 - u, & u > 0.75. \end{cases} \quad (2)$$

Here, ϵ is a small parameter that determines the low frequency of the system. The function $f(u)$ is a piecewise linear N-shaped function. The external force $\varphi(t)$ is a fast periodic pulse train with an amplitude J , period T , and pulse duration τ :

$$\varphi(t) = \begin{cases} J, & t \in [nT, nT + \tau], \\ 0, & t \in [nT + \tau, (n+1)T], \end{cases} \quad n = 0, 1, 2, \dots \quad (3)$$

Note that here we consider a case in which the period of the pulse train is much shorter than the intrinsic period of system (1): $T \ll T_{\text{int}}$.

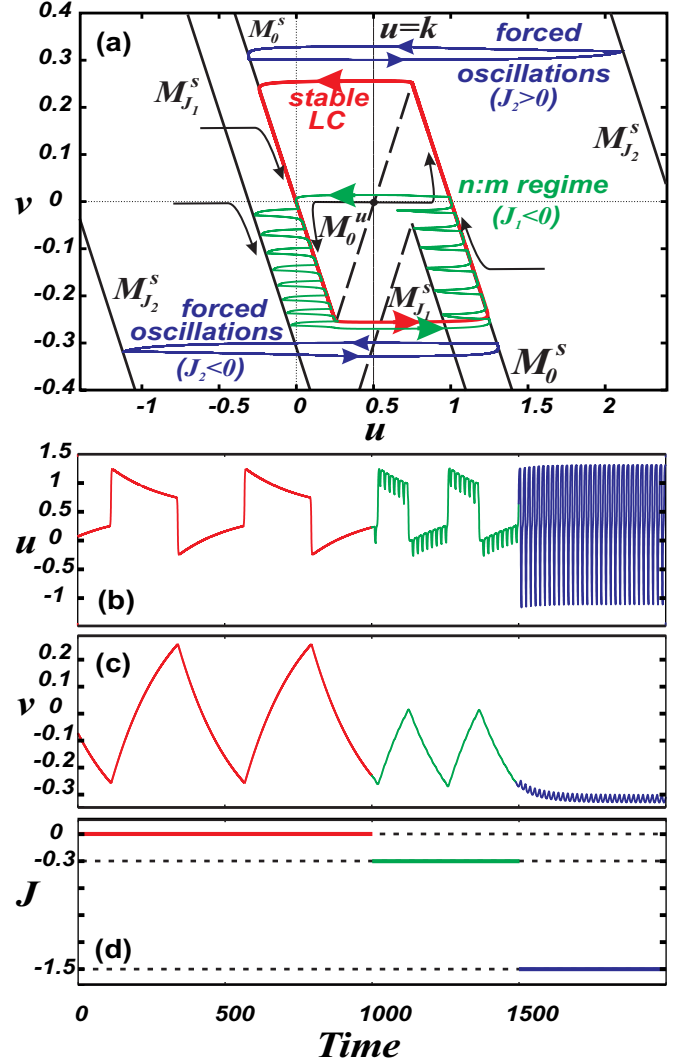


FIG. 1. Phase portrait and time series of the McKean system for $\tau = 4, T = 16, \epsilon = 0.005$. The curve marked “stable LC” (red online) corresponds to intrinsic oscillations (the unperturbed stable limit cycle, $J = 0$), the curve “n:m regime” (green trajectory and time series online) is produced by the system with weak forcing ($J_1 = 0.3$), and the curve “forced oscillations” represents the case of strong forcing ($J_2 = 1.5$; blue online). The unperturbed stable manifold of slow motion M_0^s consists of two branches: $\{v = -u, u \leq 0.25\}$ and $\{v = 1 - u, u \geq 0.75\}$, the unperturbed unstable manifold of slow motion is $M_0^u = \{v = u - 0.5, 0.25 \leq u \leq 0.75\}$. The perturbed stable slow motion manifold $M_{J_1}^s$: $\{v = -u - J, u \leq 0.25\}$ and $\{v = 1 - u - J, u \geq 0.75\}$, and the perturbed unstable slow motion manifold is $M_{J_2}^u = \{v = u - 0.5 - J, 0.25 \leq u \leq 0.75\}$. Lower panels show the time-course of the u and v variables (B and C) and changes in the amplitude parameter J (D).

III. TRANSITION TO HIGH-FREQUENCY FORCED OSCILLATIONS

We can take advantage of the small parameter $\epsilon \ll 1$ to study the dynamics of the system above using the singular perturbation theory. Without the external force $J = 0$ and for $0.25 < k < 0.75$, the system (1) has only one attractor in the phase plane—a well-studied stable relaxation limit cycle

[Fig. 1(a), red trace]. In short, it consists of two slow parts along the manifold of slow motion [right and left branches of M_0^s in Fig. 1(a), where the subscript shows the absence of the external force] and fast jumps between them.

The system displays much more complex dynamics if the forcing is nonzero: $J = J_1 \neq 0$. Let us assume for concreteness that forcing is negative $J_1 < 0$ (this corresponds to inhibitory input for the neuron). During an input pulse, the manifold of slow motion transiently moves down $M_0^s \rightarrow M_0^j$ and returns back. The fast variable u follows the slow manifold from its original to the perturbed position and back [Fig. 1(a), green trace]. Both slow parts of the relaxation limit cycle are replaced by these comblike traces. The slow variable, however, keeps progressing toward the knees of the slow manifold leading the trajectory to jump between the branches of the manifold. As soon as v falls below the left knee of the unperturbed nullcline, the trajectory jumps from the left branch to the right branch. As soon as v rises above the right branch of the perturbed nullcline, the trajectory jumps back from the upper branch to the lower branch. The trace is a typical shape of a limit cycle representing resonance between the intrinsic oscillations and forcing ($n : m$ synchronous regimes). However, in the classical case such resonance requires tight parameter tuning and occupies short intervals in the parameter space being interrupted by large quasiperiodic and chaotic windows [23,24]. In our case, the resonant windows are much wider because there are only two dominant processes—the fast oscillations and switching between the branches of the slow manifold—and both of them are determined by the same forcing.

As the forcing amplitude grows, the period of the limit cycle decreases and frequency locking occurs at lower locking numbers. The mechanism is as follows: Since the dynamics of the slow variable v contributes to the period most (fast jumps have negligible contribution), reducing the amplitude of v reduces the period most effectively. This amplitude is well approximated by the distance along v between the minimum of the manifold of slow motion in the original position M_0^s , and its maximum in the perturbed position M_0^j [Fig. 1(a)]. This distance is smaller at higher forcing amplitudes due to greater shifting of the manifold of slow motion. As a result, the amplitude of oscillations in the slow variable decreases [Fig. 1(c)], and the period does too due to the earlier jumps from M_0^j to M_0^s . The number of the forced oscillations per period of the limit cycle decreases too as the forcing amplitude grows. Eventually, the frequencies lock 1:1 [Fig. 1(a), blue]. At small enough ϵ , this occurs as the vertical location of the minimum of the original manifold M_0^s coincides with the maximum of the perturbed manifold M_0^j . Then, the slow variable does not need to change along the limit cycle, and oscillations become purely forced.

IV. ANALYSIS: THE T MAP

For (u_0, v_0) consider the trajectory $[u(t), v(t)]$ of (1) with the initial condition $[u(0), v(0)] = (u_0, v_0)$. We define the image of (u_0, v_0) by the T map as $[u(T), v(T)]$, where T is the period of the forcing φ [see Eq. (3)]. We argue that the T map decouples into one-dimensional components at lowest order. First note that at the $\epsilon = 0$ order the fast component of the map consists of the integration of the first equation of (1), with v corresponding to a constant v_0 , over the period of the forcing T . It is not

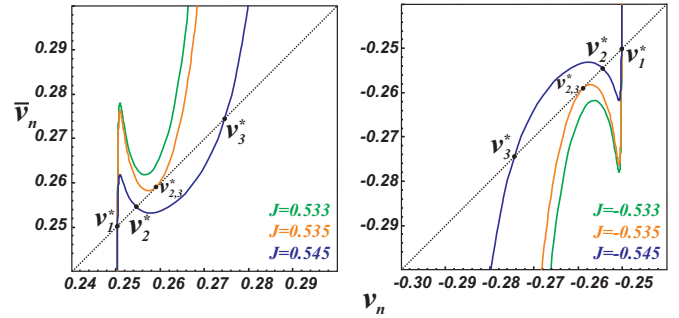


FIG. 2. The T maps for different (negative and positive) values of J ($T = 16$, $\tau = 4$, $k = 0.5$, $\epsilon = 0.005$). Stable and unstable fixed points emerge from a saddle-node bifurcation as $|J|$ increases.

hard to prove that for T sufficiently large, and for each fixed v_0 , this map has a unique stable fixed point corresponding to a periodic solution $\gamma_{v_0}(t)$ of the fast component of (1). By substituting $\gamma_{v_0}(t)$ into the slow subsystem of (1) we obtain the $O(\epsilon)$ approximation of the v component of the T map, independent of v_0 . This one-dimensional map can be written in the form

$$v \mapsto v + \epsilon P(v). \quad (4)$$

Using the piecewise-linear structure of the McKean system, we obtain an explicit formula for $\gamma_{v_0}(t)$ and hence for $P(v)$. If $J > 0$, then $P(v) = -Tv - Je^{\tau-T} \frac{(v+0.25)^2}{(v-0.25)^2} + Je^{-\tau} \frac{(0.0625+J^2+(v_n-0.5)v-J(2v-0.5))}{(0.25-J+v)^2} + \tau(1+J) - kT + \ln \frac{1}{0.25-v} + 2(v+0.25) \ln \frac{v+0.25}{v-0.25} + 2(-J+v-0.25) \ln(-J+v-0.25) - 2(-J+v-0.75) \ln(0.25+J+v)$. If $J < 0$, then $P(v) = T(1-v) - Je^{\tau-T} \frac{(v-0.25)^2}{(v+0.25)^2} + Je^{-\tau} \frac{(0.0625+J^2+(v+0.5)v-2J(v-0.25))}{(0.25-J+v)^2} + \tau(1-J) - kT + \ln(-0.25-v) + 2(v-0.25) \ln \frac{v-0.25}{v+0.25} + 2(-J+v+0.25) \ln(-J+v+0.25) - 2(-J+v+0.75) \ln(-0.25+J+v)$.

Given the decomposition of the dynamics, stability is determined by the derivative of the reduced T map defined by Eq. (4). Stable fixed points of the reduced T map correspond to persistent oscillations at the frequency of the forcing. Unstable fixed points correspond to regimes that are not observable in applications and shown here for the consistency and completeness of analysis. Fixed points of the T map are defined by the equation $P(v_n) = 0$. The point is stable if the absolute value of its multiplier is less than 1 and unstable if it is greater than 1. Thus, the stability condition is $|\epsilon \frac{\partial P}{\partial v}(v, J)|_{v=v_n} + 1| < 1$.

Since the system is symmetric, same transitions occur for J increasing from zero and decreasing from zero. To shorten the description, below we use the absolute value of J . As follows from the graph of the map and the stability condition above, for weak forcing, the T map has only one fixed point $v = v_1$, and this point is unstable (Fig. 2, green). At $|J| = J_F$ [such that $\frac{\partial P}{\partial v}(v, J_F)|_{v=v_{2,3}} = 0$] a fold bifurcation occurs and two additional fixed points emerge (Fig. 2, orange; Fig. 3, Fold), a stable and an unstable (Fig. 2, blue). The central stable fixed point $v = v_2$ corresponds to the high-frequency forced oscillations in Fig. 1. The oscillation approximated by the map implies that v remains at a constant level v_2 , and u changes in the interval $[-v_2 - J, 1 - v_2]$ with the period of forcing T . The fixed point v_2 of the T map corresponding

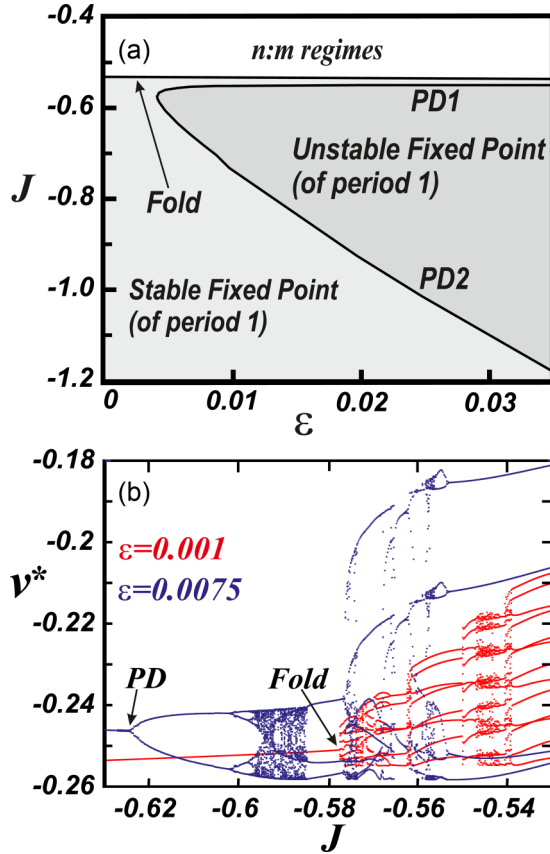


FIG. 3. (a) Two-parameter bifurcation diagram showing stability and region of existence of the fixed point of the T map. (b) One-parameter bifurcation diagram calculated numerically for the original system (1) for negative values of J ($T = 16$, $\tau = 4$, $k = 0.5$).

to this oscillation remains stable at forcing amplitudes above the bifurcation for low enough values of the small parameter ϵ . For larger values of ϵ , a period doubling bifurcation (at $J = J_{PD}$: $\epsilon \frac{\partial P}{\partial v}(v, J_{PD})|_{v=v_2} = -2$), at which the fixed point loses its stability, occurs at a forcing amplitude above the one for the fold bifurcation [Fig. 3(a)].

The explanation for the shape of the bifurcation diagram in Fig. 3(a) can be derived from the map (4). First, the fold bifurcation occurs when the map is tangent to the diagonal and, hence, $\frac{\partial P}{\partial v}(v, J_F)|_{v=v_{2,3}} = 0$. Thus, the condition is independent of ϵ (for any nonzero ϵ), and the boundary is parallel to the ϵ axis. The period doubling requires the slope of the T map to reach -1 , and the condition depends on ϵ : $[\epsilon \frac{\partial P}{\partial v}(v, J_{PD})|_{v=v_2} = -2]$. Thus, only for large enough ϵ , as the slope can reach -2 , period doubling occurs [Fig. 3(a)]. These results are in good agreement with numerical simulations [Fig. 3(b)]. In case the fixed point loses its stability, the system converges to another stable regime, which, in the case of period doubling, is also described by the T map.

V. CONCLUSIONS AND DISCUSSION

In conclusion, we want to emphasize novel features of the forced regime obtained in this work. Transition to synchronization is extensively studied in a vast number of systems. Structurally, the transition occurs through breakdown of an

invariant torus that contains the $1:n$ periodic ultraharmonics and quasiperiodic solutions [24].

We note that the mathematical explanation of the transition from $1:1$ locking to torus dynamics may involve generalized canard solutions in a similar way as in [25]. Interestingly, in our case the transition shows massive periodic regimes and very short chaotic windows in the parameter space (e.g., Fig. 3), whereas chaos is displayed much stronger in classical systems [23,24]. One explanation for the lower chaoticity in the transition is that the T map becomes a diffeomorphism at low ϵ . Another explanation is that the oscillator has a slow variable which becomes effectively a constant in the high-frequency oscillation, which renders the forced system two-dimensional and excludes the possibility of chaotic regimes. At higher ϵ , this approximation no longer holds, and, accordingly, the system shows greater chaoticity.

The timescale separation also explains the high amplitude of the fast oscillations in the forced regime: While the slow variable takes a constant value rendering the intrinsic oscillatory mechanism not functional, the fast variable is capable of following the forcing. This makes a prediction that further growth in the forcing frequency will decrease the amplitude of the forced oscillations and limit them in a range where they are insignificant for the application. For the neuron, this would mean that it is restricted in a subthreshold range and does not fire any spikes.

Overclocking of the oscillator reported here gives clear conditions necessary for it. First, the N-shaped manifold of slow motion is required not only for the slow relaxation oscillation, but also for the fast forced oscillations to have a high amplitude at moderate forcing. Forcing uses the excitability of the oscillator by moving the trajectory between the two stable branches of the manifold. Second, even though the slow variable effectively becomes a constant in the high-frequency regime, the slow equation is important as it defines the value of this variable and, thus, affects the dynamics.

The above requirements are quite general, and the high-frequency forced response can be obtained in a wide range of systems, yet the effect is not trivial. To emphasize that, we note that in a range of models the high-frequency forced response is not represented correctly or even possible. The trajectory of the forced oscillation does not belong to a neighborhood of the original low-frequency limit cycle. Thus, all models that assume that trajectories do not leave the vicinity of the limit cycle of the unforced system, such as phase oscillator and phase response method, are unable to reproduce the transition to forced oscillations. On the other hand, integrate and fire models not only have no intrinsic frequency, but are also built for weak inputs, which require summation (integration) to produce a spike. Thus, our model fills the gap between these options and provides a highly reduced model that replicates both low- and high-frequency oscillations, as well as the transition between them.

Inside the parameter region where the $1:1$ periodic solution exists, the solution may lose stability via a period doubling bifurcation. While this bifurcation is typical, especially for higher harmonics, here the $1:1$ solution loses stability in period doubling for greater values of the small parameter ϵ . This means that the instability occurs for smaller frequency mismatch between the forcing and the natural frequency of

the oscillator (which is determined by ϵ). Full analysis of the transition is a subject of future research.

We found this transition to high-frequency oscillations in a conductance-based model of neurons [17], and we believe that additional applications will be found once we describe the phenomenon. In neuroscience, the analyzed system presents a neuron under the influence of a pulsatile forcing. We have shown that by this mechanism, contrary to the intuition, a classical inhibitory (hyperpolarizing) input can increase the frequency of a downstream neuron, i.e., excite them instead of inhibiting them [17]. We have shown that the conditions for the frequency increase are physiologically plausible. In particular, the formation of the pulsatile input requires synchronization among the neurons forming the input, and we have shown that synchrony in several neuronal populations, including one recorded by us, exceeds that required for the transition to the high frequency. Additionally, we emphasize that the amplitude of this forcing is not required to be high, but stays at the level of other terms in the system. Thus, forcing uses excitability of the oscillator as opposed to completely destroying its internal dynamics. As a result, the amplitude of the forced oscillation remains high in spite of a great difference in the frequencies. We further believe that the

phenomenon we describe here can be applied to analyze neuronal synchrony in the gamma oscillatory range: where the pyramidal neurons, which have a relatively slow intrinsic rhythm, are forced by rapidly firing fast inhibition [26,27]. In this case, as our previous analysis suggested, the pyramidal neurons are synchronized by the pulsatile inhibitory inputs to the faster gamma rhythm [28]. In summary, the phenomenon that we describe herein should be generically applicable to a wide variety of cross-frequency coupled systems with pulsatile coupling.

ACKNOWLEDGMENTS

This work was partially supported by the Russian Foundation for Basic Research (Grant No. 17-02-00874). A.K. was supported by NIH NIAAA Grant No. R01AA022821. M.K. was supported in part by the ERC Advanced Grant NerVi No. 227747. B.G. was supported by the LABEX ANR-10-LABX-0087 IEC and IDEX ANR-10-IDEX-0001-02 PSL* and also acknowledges the RF academic excellence Program 5-100. D.Z. acknowledges support of Russian Science Foundation Grant No. 18-11-00294 (numerical simulations).

-
- [1] A. Pikovsky, M. Rosenblum, and J. Kurths, *Synchronization. A Universal Concept in Nonlinear Sciences* (Cambridge University Press, Cambridge, 2001).
 - [2] F. M. Gardner, *Phase-lock Techniques* (Wiley, NJ, 2005).
 - [3] F. A. Rodrigues, T. K. DM. Peron, P. Ji, and J. Kurths, *Phys. Rep.* **610**, 1 (2016).
 - [4] G. Buzsaki, *Rhythms of the Brain* (Oxford University Press, Oxford, 2006).
 - [5] S. N. Rasband, *Chaotic Dynamics of Nonlinear Systems* (Wiley, New York, 1990).
 - [6] F. C. Hoppensteadt and E. M. Izhikevitch, *Weakly Connected Neural Networks* (Springer-Verlag, New York, 1997).
 - [7] A. T. Winfree, *The Geometry of Biological Time* (Springer-Verlag, Berlin, 2001).
 - [8] M. R. Guevara and L. Glass, *J. Math. Biol.* **14**, 1 (1982).
 - [9] I. Ratas and K. Pyragas, *Nonlinear Dyn.* **67**, 2899 (2012).
 - [10] L.-Y. Wang and L. K. Kaczmarek, *Nature (London)* **394**, 384 (1998).
 - [11] M. Kivela *et al.*, *J. Complex Netw.* **2**, 203 (2014)
 - [12] S. Li, S. Stokes, Y. Liu, S. Foss-Schroder, W. Zhu, and D. Palmer, *J. Appl. Phys.* **91**, 7346 (2002).
 - [13] K. L. Kilgore and N. Bhadra, *Med. Biol. Eng. Comput.* **42**, 394 (2004).
 - [14] L. Garcia *et al.*, *Trends Neurosci.* **28**, 209 (2005).
 - [15] B. Guse, P. Falkai, and T. Wobrock, *J. Neural. Transm.* **117**, 105 (2010).
 - [16] K.-M. Lee *et al.*, *New J. Phys.* **14**, 033027 (2012).
 - [17] E. O. Morozova, M. Myroshnichenko, M. di Volo, B. Gutkin, C. Lapish, and A. Kuznetsov, *J Neurophysiol.* **116**, 4 (2016).
 - [18] K. Diba, A. Amarasingham, and K. Mizuseki, *J. Neurosci.* **34**, 14984 (2014).
 - [19] M. Izhikevich, *Dynamical Systems in Neuroscience: The Geometry of Excitability and Bursting* (MIT Press, Cambridge, 2007).
 - [20] A. Hyafil, A.-L. Giraud, L. Fontolan, and B. Gutkin, *Trends Neurosci.* **38**, 725 (2015).
 - [21] Y. Kuznetsov, *Elements of Applied Bifurcation Theory*, 3rd ed. (Springer-Verlag, Berlin, 2004).
 - [22] H. P. McKean, *Adv. Math.* **4**, 209 (1970).
 - [23] N. Inaba and S. Mori, *IEEE Trans. Circuits Syst.* **38**, 398 (1991).
 - [24] M. Sekikawa *et al.*, *Int. J. Bifurcation Chaos* **18**, 1051 (2008).
 - [25] M. A. Kramer, R. D. Traub, and N. J. Kopell, *Phys. Rev. Lett.* **101**, 068103 (2008).
 - [26] X. J. Wang, *Physiol. Rev.* **90**, 1195 (2010).
 - [27] M. Bartos *et al.*, *Proc. Natl. Acad. Sci. USA* **99**, 13222 (2002).
 - [28] A. Hyafil *et al.*, *eLife* **4**, e06213 (2015).